UCSF
UC San Francisco Previously Published Works

Title

Dark-Adaptation Functions in Molecularly Confirmed Achromatopsia and the Implications for Assessment in Retinal Therapy TrialsDark-Adaptation Functions in Achromatopsia

Permalink

Journal

ISSN

Authors

Aboshiha, Jonathan
Luong, Vy
Cowing, Jill
et al.

Publication Date

2014-10-10

DOI

Peer reviewed

Dark-Adaptation Functions in Molecularly Confirmed Achromatopsia and the Implications for Assessment in Retinal Therapy Trials

Jonathan Aboshiha,[1,2] Vy Luong,[1] Jill Cowing,[1] Adam M. Dubis,[1,2] James W. Bainbridge,[1,2] Robin R. Ali,[1] Andrew R. Webster,[1,2] Anthony T. Moore,[1,2] Frederick W. Fitzke,[1] and Michel Michaelides[1,2]

[1]UCL Institute of Ophthalmology, University College London, London, United Kingdom
[2]Moorfields Eye Hospital, London, United Kingdom

PURPOSE. To describe the dark-adaptation (DA) functions in subjects with molecularly proven achromatopsia (ACHM) using refined testing conditions with a view to guiding assessment in forthcoming gene therapy trials.

METHODS. The DA functions of nine subjects with ACHM were measured and compared with those of normal observers. The size and retinal location of the stimuli used to measure DA sensitivities were varied in four distinct testing condition sets, and the effect of altering these parameters assessed.

RESULTS. In three of the four testing condition sets, achromats had significantly higher mean final thresholds than normal observers, whereas in the fourth condition set they did not. A larger, more central stimulus revealed the greatest difference between the final DA thresholds of achromat and normal subjects, and also demonstrated the slowest rate of recovery among the achromat group.

CONCLUSIONS. In this, the largest study of DA functions in molecularly proven ACHM to date, we have identified optimal testing conditions that accentuate the relative difference between achromats and normal observers. These findings can help optimize DA testing in future trials, as well as help resolve the dichotomy in the literature regarding the normality or otherwise of DA functions in ACHM. Furthermore, the shorter testing time and less intense adaptation light used in these experiments may prove advantageous for more readily and reliably probing scotopic function in retinal disease, and be particularly valuable in the frequent post therapeutic assessments required in the context of the marked photophobia in ACHM.

Keywords: achromatopsia, dark adaptation, gene therapy, rod monochromatism, rod vision

Achromatopsia (ACHM) is an autosomal recessive cone dysfunction syndrome, with an incidence of 1 in 30,000, and is characterized by the presentation in infancy of nystagmus, poor visual acuity, and photophobia.[1] Electroretinography (ERG) testing classically demonstrates absent cone responses and normal or near-normal rod responses.[2,3]

To date, sequence variants in five genes have been associated with ACHM: *CNGA3*, *CNGB3*, *GNAT2*, *PDE6C*, and *PDE6H*.[4–8] All five genes encode components of the cone-specific phototransduction cascade, with *CNGA3* and *CNGB3* together accounting for approximately 70% to 80% of ACHM,[9] while the remaining three genotypes are responsible for less than 2% of cases.[6–8]

Recently, several studies have demonstrated the effectiveness of using gene replacement to restore cone function in various animal models of ACHM,[10–13] and the neuroprotective protein ciliary neurotrophic factor (CNTF) has also been shown to induce a transient restoration of cone ERG responses and visually directed behavior in the *CNGB3* dog model.[14] Given these promising results, human clinical trials are expected in the near future, making the accurate measurement of retinal function in ACHM critical in terms of monitoring treatment response.

Dark-adaptation (DA) function measurements are one means of measuring retinal function that will likely feature in anticipated trials for ACHM. Such measurements can yield important information about photoreceptor function, in particular that of the rods, both prior to treatment and as a means of monitoring treatment effect.

The DA function curve is used to study the gain in retinal sensitivity after a change from photopic to scotopic ambient lighting conditions. It is classically described in normal observers as a biphasic curve of reducing visual threshold intensity over time, with an initial phase of cone-mediated increased sensitivity followed by a more prolonged rod-mediated phase; the two phases being separated by a point in the dark-adaptation curve called the cone-rod break.[15] After bleaching of the visual pigment, there is a subsequent time-dependent increase in retinal sensitivity in scotopic conditions, as the photosensitive pigment is restored; this constitutes the physiological process of DA. This increase in sensitivity over time to increasingly dimmer stimuli is related to the amount of opsin regenerated.[15]

The DA curves measured in ACHM provide data on rod system function, which has classically been described as

essentially normal, based predominantly on ERG and psychophysical assessments.[2,16,17] The importance of monitoring rod function in treatment trials has been illustrated in animal models, with CNTF treated *CNGB3* dogs demonstrating a transient decrease in rod ERG responses.[14] Therefore, it is important to know how these functions differ between the achromat and the normal observer, and in this regard the literature is conflicting. This dichotomy can be broadly classified by observations that: (1) achromats have DA curves that are the same as the rod component of the normal observers' DA curves,[3,18–21] or (2) achromats have DA curves whose thresholds are elevated compared with those of normal observers.[22–24]

Simunovic et al.[22] observed that the final thresholds in the four achromats (not molecularly proven) that they tested were significantly elevated compared with those of normal observers. In contrast, Nordby et al.[18] state that, in their study of one achromat, the DA threshold curves (measured 7° nasally) "followed exactly the same course as those of the normal subject." Of interest, Hess et al.[25] found that the recovery in sensitivity after DA, which they observed in two S-cone monochromats also was very similar to that of normal observers. However, Frey et al.[24] found that the final threshold of the mean DA curve of 10 complete achromats was slightly elevated (by 0.1 log unit) compared with normal observers, although they felt this might be explained by the fact that six of these subjects were children whose concentration may have been suboptimal.

There is also disagreement in the literature about the shape of the DA curves measured. Given the assumption that complete achromats have no functioning cones,[19,26–29] it might be anticipated that DA curves would follow a monophasic curve due to the gain in sensitivity in rod function alone over time, and this has indeed been reported.[30] In contrast, however, Sloan[23] asserted that 11 of the 14 complete achromats that she tested had DA curves in which there was evidence that receptors other than normal rods were functioning. A significant limitation of all of these studies was that the diagnosis of ACHM was made only by the presence of clinical features and color vision tests, and the absence of electrophysiological and molecular genetic evidence must be borne in mind. In a further study by Sloan and Feiock,[31] although two of the four complete achromats tested had monophasic DA curves, two others had biphasic curves. This was interpreted as further evidence for the existence of 'photopic rods,' which had the spectral sensitivity of rhodopsin but, in the light-adapted eye, had lower thresholds than normal rods.[26] However, it is not made clear how the diagnosis of complete ACHM was reached. Farkas et al.[32] did report two cases of genetically confirmed ACHM, where their *CNGB3* patient tested had a monophasic dark-adaptation curve, contrasting with an abnormal biphasic curve seen in their *CNGA3* patient.

Most of the literature to date on DA functions in ACHM has relied on a psychophysical, clinical, and/or electrophysiological diagnosis. To the best of our knowledge, we present the largest series in the literature to date concerning DA data measured in molecularly-proven patients. Furthermore, we have investigated a variety of testing conditions to establish an optimal protocol for use in ACHM and also to more readily and efficiently probe scotopic function in other retinal disease subject to intervention.

METHODS

Subjects

Nine patients with typical clinical and electrophysiological findings (including no evidence of any cone function in the form of flicker or photopic ERG responses) of complete ACHM were ascertained. All underwent a clinical history and detailed ocular examination, including best-corrected visual acuity (BCVA) using an Early Treatment Diabetic Retinopathy Study chart, and color vision testing using the Ishihara and Hardy Rand Rittler (HRR) pseudoisochromatic plates. Six subjects with normal vision (i.e., unaided visual acuity [VA] or BCVA $\leq$ logMAR 0), normal color vision (Ishihara and HRR plates), and no ocular pathology were recruited as normal controls. The study protocol adhered to the Tenets of the Declaration of Helsinki, and was approved by the Moorfields Eye Hospital ethics committee (London, UK). Informed consent was obtained from all subjects before entering the study.

Dark-Adaptation Measurements

Dark adaptation was measured using a modified Humphrey Visual Field Analyzer Model 610 (Humphrey Instruments, San Leandro, CA, USA), for use under scotopic conditions. This was controlled by an external computer (PS/2 model 50; International Business Machines, Armonk, NY, USA) using a custom program running Qbasic Software (Microsoft, Redmond, WA, USA). The subject was seated at the field analyzer, with their head position controlled by a chin and forehead rest, 30 cm from the fixation target. Prior to commencing the test, the task was demonstrated to the subjects and they were allowed a brief practice in order to familiarize themselves with the procedure. The eye to be tested was then dilated using 1% wt/vol tropicamide eye drops, and the nontested eye was covered. Subjects were then instructed to look at a red fixation light while the Humphrey background light of 2.8 log scotopic td was left on for 20 minutes, achieving an equilibrium bleach of approximately 2% of the available rhodopsin.

Prior to this light intensity being chosen, two brighter light adaptation levels had been trialed; one with a 2-minute period of very bright light adaptation using lamps installed in the Humphrey perimeter (equivalent to 7.5 log scotopic td-s), which was sufficient to bleach more than 95% of rhodopsin,[33] and a second with this same light intensity reduced by a 0.6 neutral density filter. However, both these brighter lighting conditions caused unacceptable discomfort to the considerably photophobic ACHM subjects, who were unable to maintain eye opening for effective light adaptation. The Humphrey background level was subsequently chosen because it approximates the minimum brightness for photopic cone–dependent vision,[34] but was also of an intensity level that was tolerable by the ACHM patients. In addition to reducing discomfort, the lower intensity adaptation light also had the advantage of allowing observations to be made of the earlier phase of the rod DA curve in normal subjects, which would otherwise be determined by cones in stronger light-adaptation conditions,[35] as well as importantly reducing the testing time required to reach final threshold sensitivities.[36] Both the comfort of the subjects during testing, and the time taken to measure the DA functions, are important factors to consider when designing DA measurement protocols for potential treatment trials, in which affected individuals, including children, may need frequent repeated testing over a sustained period of follow-up.

After 20 minutes of light adaptation, the light was turned off and the test begun in complete darkness. An infrared source illuminated the perimetry bowl, and an infrared camera (Phillips, Eindhoven, the Netherlands) was used to monitor eye movement and to align the tested eye.

The Humphrey stimulus light was passed through a 500-nm short pass filter and an additional 1.3-log unit neutral density filter was manually inserted to extend the measurement range. Stimulus duration was 200 msec and measured at one of two retinal locations; either displaced 3° horizontally and 3°

TABLE 1. Demographics, VA, and (Where Applicable) Genotype of the ACHM Subjects (Designated With a Number) and Normal Subjects (Designated With a Letter) Who Underwent Dark-Adaptation Testing

Subject	Age, y/Sex	BCVA OD, logMAR	BCVA OS, logMAR	Gene	Allele 1/Allele 2
1	14/f	0.86	0.90	*CNGB3*	c.1148delC-p.Thr383Ile fs*13/c.1006G>T-p.Glu336Ter
2	20/m	0.88	0.74	*CNGB3*	c.595delG-p.Glu199Ser fs*3/c.1148delC-p.Thr383Ile fs*13
3	28/m	1.00	1.20	*CNGB3*	c.1148delC-p.Thr383Ile fs*13/c.1853delC-p.Thr618Ile fs*2
4	37/m	0.82	0.88	*CNGB3*	c.1148delC-p.Thr383Ile fs*13/c.1148delC-p.Thr383Ile fs*13
5	48/m	0.92	0.96	*CNGB3*	c.1148delC-p.Thr383Ile fs*13/c.1148delC-p.Thr383Ile fs*13
6	32/m	0.74	0.90	*CNGA3*	c.848G>A-p.Arg283Gln/c.667C>T-p.Arg223Trp
7	49/f	1.00	1.04	*CNGA3*	c.67C>T-p.Arg23Ter/c.67C>T-p.Arg23Ter
8	54/f	1.02	1.04	*CNGA3*	c.1641C>A-p.Phe547Leu/c.1641C>A-p.Phe547Leu
9	51/f	0.96	0.94	*GNAT2*	c.843-844insAGTC-p.His282Ser fs*11/c.843-844insAGTC-p.His282Ser fs*11
a	30/m	≤0	≤0	~	~
b	32/m	≤0	≤0	~	~
c	34/m	≤0	≤0	~	~
d	34/m	≤0	≤0	~	~
e	34/f	≤0	≤0	~	~
f	40/m	≤0	≤0	~	~

BCVA, best-corrected visual acuity; f, female; m, male; OD, right eye; OS, left eye.

vertically from fixation (3,3), or displaced 9° horizontally and 9° vertically (9,9). Two stimuli were used; Goldmann size III (0.43° diameter) and Goldmann size V (1.72° diameter). The subject was asked to press a response button when they detected a flash. The initial flash intensity was set at 25 db and increased in 5-db steps until seen by the subject, at which point this was recorded as the initial threshold intensity. This was first done for the Goldmann size III stimulus at location 3,3, then for the Goldmann size V stimulus at the same location, and subsequently for the Goldmann size III at 9,9 and Goldmann size V at 9,9. The thresholds were then measured for these four conditions repeating in this order, during one period of dark adaptation. The testing strategy used a method of ascending limits, and after each response the stimulus intensity for each size and location was reduced by 7 dB for the first three responses, and by 3 dB for subsequent responses. The stimulus was then increased in 1-dB steps until the subject recorded a response. The DA responses were recorded for at least 20 minutes in all subjects tested, which given the low rhodopsin bleach was sufficient to reach plateau sensitivities.[36]

Molecular Genetic Testing

Conventional direct Sanger sequencing of exons and exon-intron boundaries of *CNGA3*, *CNGB3*, *GNAT2*, and *PDE6C* was undertaken using previously published methods.[6,9,37]

Data Analysis

The following equation for a single-phase exponential curve (GraphPad Software, Inc., La Jolla, CA, USA) was used to fit the DA data:

$$Y = (Y0 - Plateau) \times \exp(-K \times X) + Plateau \qquad (1)$$

where Y = threshold (dB); $Y0$ = threshold intensity (dB) when time is zero; X = time (minutes); K = the rate constant (inverse minutes); and *Plateau* = final threshold (dB).

A single-phase decay curve was fitted to both the normal and ACHM data to derive the final thresholds. It has been previously shown that with similarly low light-adaptation intensities, the measured DA curves in normal observers assume a monophasic shape.[36] By way of a sensitivity analysis, in order to verify that these final threshold sensitivities were only derived from rod photoreceptors, we repeated the analysis for all conditions in all normal subjects and achromats, using only data acquired after 15 minutes of dark adaptation. After this time it can be reasonably assumed that only rod function kinetics were contributing to the change in recorded sensitivities, as cones typically fully dark-adapt within 3 to 6 minutes, while rods take at least 20 minutes to achieve their final dark-adapted level, depending on the intensity of the adaptation light.[20,38,39] A linear regression was fitted to the post 15-minute data (GraphPad Software, Inc.), and the resulting thresholds at 30 minutes post adaptation for each eye in the normal subjects and achromats calculated, in each of the four testing condition combinations (i.e., Goldmann size III and V stimuli in positions 3,3 and 9,9). Histogram plots and the D'Agostino and Pearson omnibus normality test were used to verify the normality of data before the use of any parametric tests. Statistical analyses were performed using GraphPad Prism, version 5 (GraphPad Software, Inc., La Jolla, CA, USA).

RESULTS

The normal cohort had a mean age of 34 years (range, 30–40 years), which was not significantly different to the mean age in the ACHM cohort of 37 years (range, 14–54 years) (unpaired *t*-test; $P = 0.63$). Five of the nine ACHM patients were male (56%), as were five of the six normal subjects (83%). All normal subjects had a monocular unaided VA or BCVA in each eye of logMAR 0 or better. The ACHM patients had a mean monocular BCVA of 0.93 logMAR (range, 0.74–1.2). A summary of the demographics, VA, and genotype of all subjects tested is shown in Table 1. All ACHM subjects were able to read the Ishihara demonstration plate, but were unable to read any of the subsequent screening or diagnostic plates, or any of the HRR screening and diagnostic plates.

Dark Adaptation

Table 2 shows the final DA thresholds derived from the exponential curve fits for the nine ACHM patients, in each of the two locations tested (3° lateral and 3° superior from fixation, and 9° lateral and 9° superior) and for the two stimuli sizes used (Goldmann size III [0.4°] and Goldmann size V [1.7°]).

There was no statistically significant difference in final thresholds between the left and right eyes of achromats, and

TABLE 2. The Final Dark-Adaptation Thresholds (in dB) for Nine ACHM Subjects, in Each of the Two Locations Tested (3° Lateral and 3° Vertical From Fixation, and 9° Lateral and 9° Vertical) and for the Two Stimuli Sizes Used (Goldmann Size III [0.4°] and Goldmann Size V [1.7°])

| | Position 3,3 | | | | Position 9,9 | | | |
| | Size III | | Size V | | Size III | | Size V | |
Subject	OD	OS	OD	OS	OD	OS	OD	OS
1	11.4	15.9	9	10.2	2.7	6	0.3	1
2	10.4	7.1	4.2	6.4	4.7	4.6	0.5	0.4
3	10.9	13.7	11.4	11.8	1.8	3.7	1.2	2
4	19.7	12.8	14.9	13.4	7.5	3.8	3.5	3.5
5	17	17.1	13.4	14.6	7.4	7.4	3.2	6.7
6	18.3	9.2	17	16.5	8	6	5.8	6.3
7	27.9	23.4	28.2	18.4	16.1	11.6	9.6	7.2
8	26.2	24.7	17	14.9	12.1	8.7	6	4
9	12.4	14.8	7.4	7.7	2.6	2.5	−1.3	−0.6

The method of derivation of the final thresholds is described in the text. OD, right eye; OS, left eye.

between the left and right eyes of normals, in each of the four testing conditions (paired *t*-test; achromats: 3,3 position, size III stimulus [$P = 0.30$], and size V [$P = 0.45$]; and 9,9 position, size III [$P = 0.31$], and size V [$P = 0.75$]; normals: 3,3 position, size III [$P = 0.81$], and size V [$P = 0.86$]; and 9,9 position, size III [$P = 0.88$], and size V [$P = 0.47$]). The mean of the left and right eye final thresholds was then calculated for each subject in each of the four testing conditions, and used for further analysis.

These final thresholds derived from the single-phase exponential curve fit were compared with the post 15-minute data analyses for all subjects in all conditions, and were not found to be significantly different in any of the testing combinations (paired *t*-test; achromats 3,3 position, size III [$P = 0.25$], and size V [$P = 0.39$], and 9,9 position size III [$P = 0.61$], and size V [$P = 0.16$]; normals 3,3 position, size III [$P = 0.41$], and size V [$P = 0.22$], and 9,9 position, size III [$P = 0.51$], and size V [$P = 0.19$]). Figure 1 shows the dark-adaptation curves for 18 eyes in the 9 achromats versus 12 eyes in the six normal observers, in each of the four testing conditions.

When comparing the mean of the right and left eye final thresholds, the ACHM patients had statistically significantly higher mean final thresholds than normal subjects in all conditions tested (indicated with an asterisk in Fig. 1), except
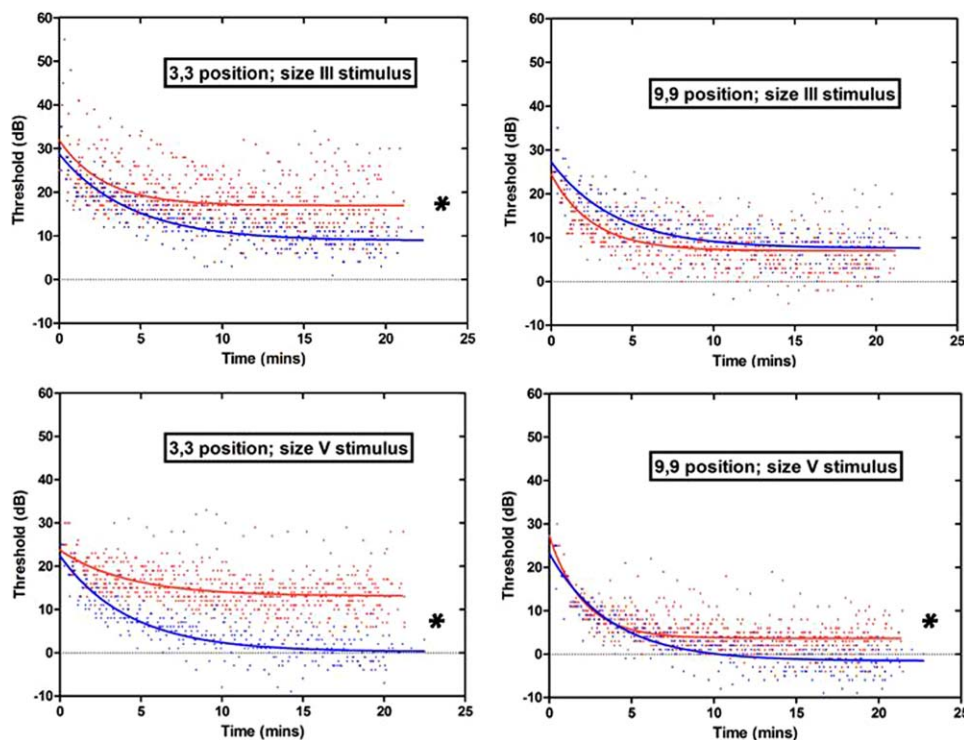

FIGURE 1. The DA curves of ACHM patients (*red data points* and exponential curve fit) and normal subjects (*blue data points* and exponential curve fit) in each of the four testing conditions. *Top row*: Goldmann size III stimulus (0.4°); *bottom row*: Goldmann size V stimulus (1.7°). *Left column*: stimulus presented at a position 3° lateral and 3° vertical from fixation; *right column*: stimulus presented at 9° lateral and 9° vertical from fixation. The ACHM patients have statistically significantly higher mean final thresholds than normal subjects (indicated with an *asterisk*) at the more central location tested with both stimulus sizes, and at the more peripheral location with the size V stimulus, see text for *P* values.

TABLE 3. The Mean Final Thresholds (dB) for All Achromat (Bold Figures Above Diagonal) and Normal Subjects (Regular Figures Below Diagonal) in Each of the Four Testing Conditions, as Indicated by Row Title (Goldmann Stimulus Size) and Column Title (Horizontal and Vertical Displacement [deg] of Stimulus From Fixation)

	Position 3,3	Position 9,9
Size III	**16.3 *** / 8.4	**6.5** / 7.0
Size V	**13.1 *** / -0.3	**3.3 *** / -1.9

* Statistically significant difference between achromat and normal subjects (see text for *P* values).

FIGURE 2. A plot of the difference between the mean final dark-adapted thresholds of achromat versus normal subjects (i.e., achromat final threshold minus normal final threshold) in each of the four testing conditions, as indicated by position (horizontal and vertical displacement [deg] of stimulus from fixation) and stimulus size (Goldmann). Positive values indicate that achromats have higher thresholds than normals, and negative values indicate that they have lower thresholds. Conditions whose threshold differences reach statistical significance are indicated with an *asterisk*. There appears to be a gradation of conditions that extenuate the difference between achromat and normal mean final thresholds, with the difference being most marked with a larger, more central stimulus.

for at the 9,9 position with the size III stimulus (unpaired *t*-test; 3,3 size III *P* = 0.007; 3,3 size V *P* = 0.0001; 9,9 size III *P* = 0.79; 9,9 size V *P* = 0.004). The comparison of achromat versus normal subjects' final thresholds was also carried out between right eyes and left eyes separately in all testing conditions, and there was no difference in terms of which condition sets revealed a statistically significant difference between the groups (unpaired *t*-test; Right eyes: 3,3 size III *P* = 0.007; 3,3 size V *P* = 0.0005; 9,9 size III *P* = 0.96; 9,9 size V *P* = 0.013. Left eyes: 3,3 size III *P* = 0.021; 3,3 size V *P* < 0.0001; 9,9 size III *P* = 0.61; 9,9 size V *P* = 0.004). For all analyses of only right eyes, only left eyes, or the mean data from both eyes, the achromats had statistically significantly higher final thresholds in all conditions tested except position 9,9 stimulus size III (Table 3). This difference between mean final thresholds of the achromats and the normal subjects was most marked in the 3,3 position with the size V stimulus, where the mean final threshold of all the achromats was 13.4 dB higher than in the normal subjects (13.1 dB and −0.30 dB, respectively; Table 3).

The plot in Figure 2 shows the differences between the mean final thresholds measured in the achromats and the normal subjects, calculated as achromat final threshold minus normal final threshold. There appears to be a reduction in the difference between the achromat and normal final threshold means with progression across the different testing conditions. The stimulus location appears to have the greatest effect in differentiating the normal and achromat groups in terms of their final thresholds (i.e., with a more central stimulus location the difference between groups was more marked than with either target size in the more peripheral location). The only condition set where no statistical difference was found between the achromat and normal observer groups (i.e., position 9,9 size III) is opposite, in terms of both stimulus location (more peripheral) and stimulus size (smaller), to the condition set where the difference was most pronounced (i.e., position 3,3 size V).

We also compared the rate constants observed in the achromats with those observed in the normal cohort, in each of the four testing condi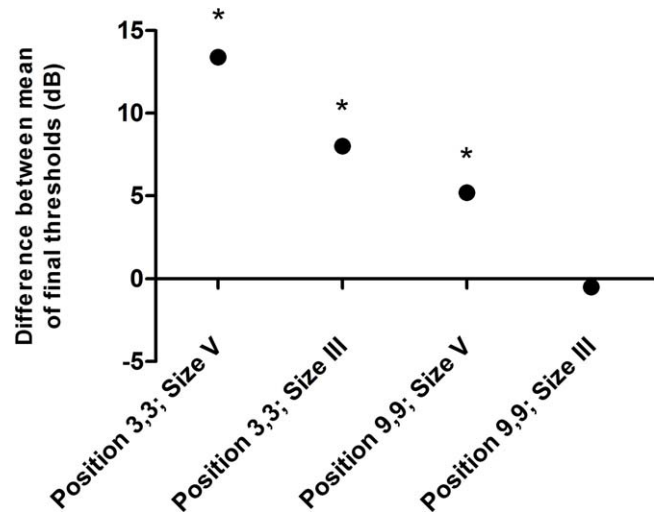tions. The mean of the right and left eye rate constants were calculated for achromat and normal subjects in all four testing conditions. The achromats had significantly higher rate constants (indicating a steeper dark-adaption curve and faster recovery of sensitivity) in three of the four testing condition sets, the exception being position 3,3 size V, where they were not significantly different (Mann-Whitney *U* test; 3,3 size III *P* = 0.015; 3,3 size V *P* = 0.228; 9,9 size III *P* = 0.012; 9,9 size V *P* = 0.001; Table 4). This was in direct contrast with mean final threshold measurements, where position 3,3 size V demonstrated the greatest difference between achromats and normals (Fig. 2).

Figure 3 shows the final thresholds plotted against the rate constant for each of the nine ACHM subjects, in each of the four condition sets tested. The 95% confidence interval (CI) for the mean value of these two parameters in normals is shown for comparison (checkered ellipse). Among the achromat group there was no statistically significant correlation between final threshold and rate constant in position 3,3 size III (Spearman *r* = 0.68; *P* = 0.0503), position 3,3 size V (Spearman *r* = 0.67; *P* = 0.06), and position 9,9 size V (Spearman *r* = 0.53; *P* = 0.148). However, in position 9,9 size III there was a statistically significant correlation between these two parameters (Spearman *r* = 0.72; *P* = 0.037).

Molecular Genetics and Genotype Correlation

Five ACHM patients (56%) had disease-causing sequence variants identified in *CNGB3*, three patients (33%) in *CNGA3*, and one patient (11%) in *GNAT2* (Table 1). This roughly approximates the population prevalence distribution of these genotypes in ACHM (*CNGB3* at 50%,[40] *CNGA3* at 25%,[41] and *GNAT2* at <2%[6]). The detailed in silico analysis of these previously described variants has been published.[9,41-45] There was no statistically significant difference in the final thresholds or the rate constants between the three genotypes in each of

TABLE 4. The Average Rate Constants (Inverse Minutes) for All Achromat (Bold Figures Above Diagonal) and Normal Subjects (Regular Figures Below Diagonal) in Each of the Four Testing Conditions, as Indicated by Row Title (Goldmann Stimulus Size) and Column Title (Horizontal and Vertical Displacement [deg] of Stimulus From Fixation)

	Position 3,3	Position 9,9
Size III	**0.40 *** / 0.22	**0.49 *** / 0.28
Size V	**0.26** / 0.23	**0.55 *** / 0.26

The larger the numeric value, the faster the recovery in sensitivity.
* Statistically significant difference between achromats and normals (see text for *P* values).

the four testing conditions (Kruskal-Wallis test with Dunn's Multiple Comparison test; $P < 0.05$ for all genotype cross-comparisons in all four condition sets).

DISCUSSION

This study demonstrates that molecularly proven achromats have significantly higher final DA thresholds than normal observers in three of the four conditions tested. A larger, more central stimulus appears to reveal the greatest difference between the final DA thresholds of the achromats and normal subjects. To the best of these authors' knowledge, this is the largest published series to date of DA function data in molecularly proven ACHM (PubMed search 05/20/2014; keywords: achromatopsia, rod monochromatism, dark adaptation). That the final thresholds calculated from our exponential curve fits were not significantly different from the final thresholds as calculated by our post 15-minute analysis is also in keeping that these thresholds were derived from changes in rod function alone. Our data is in agreement with those studies, which indicated that achromats have elevated thresholds compared with normal observers,[22–24] and provides some evidence that the assumption that achromats have normal DA final threshold sensitivities may not be correct, at least in three of the four testing conditions employed herein.

However, it is also of note that in one of the four condition sets tested there was no statistically significantly difference between the achromat and normal group final DA thresholds. This effect of location and stimulus size on the relative difference between normal and achromat observers may partly
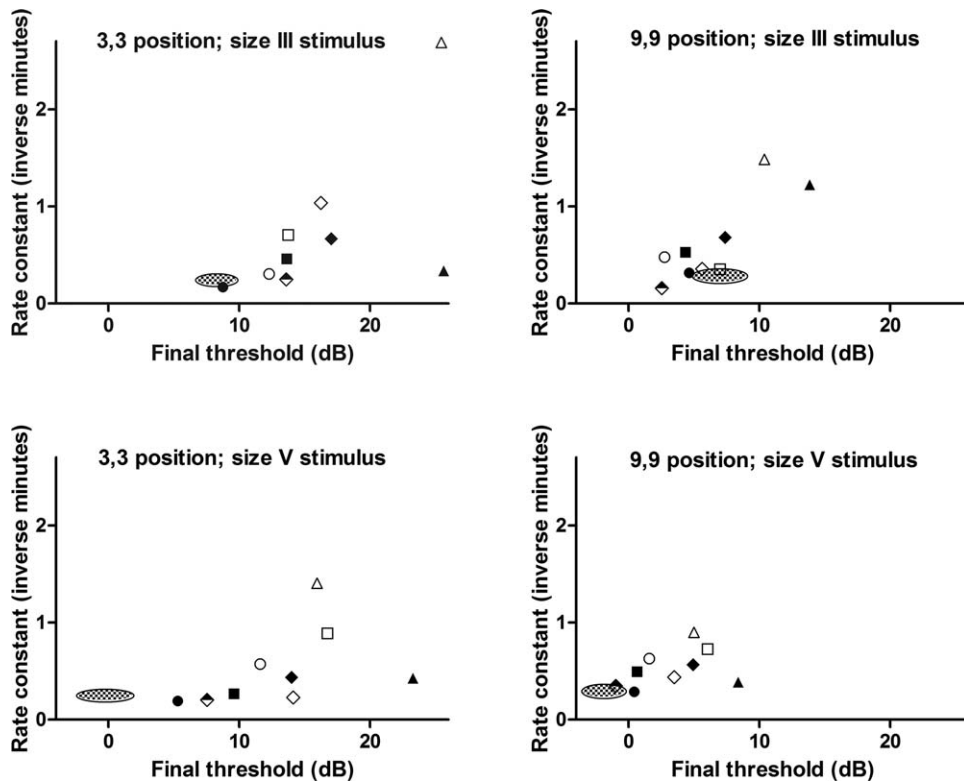

FIGURE 3. Plots showing the nine individual ACHM subjects' rate constant (inverse minutes) versus final threshold (dB), in each of the four condition sets tested (indicated by *plot title*). The 95% CI for the mean of these parameters measured in the normal subjects is shown for comparison (*checkered ellipse*). There is a statistically significant positive correlation between final threshold and rate constant in one of the four condition sets tested (9,9 position, size III stimulus; Spearman $r = 0.72$; $P = 0.037$), see text for further discussion. Subject key: Subject 1, *filled square*; Subject 2, *filled circle*; Subject 3, *empty circle*; Subject 4, *empty diamond*; Subject 5, *filled diamond*; Subject 6, *empty square*; Subject 7, *filled triangle*; Subject 8, *empty triangle*; Subject 9, *half-filled diamond*.

account for the divergence of observations in the literature. In both achromats and normal subjects, the final DA thresholds measured were lowest for the more peripherally located and larger stimuli. This finding is physiologically plausible. The latter observation would be due to the increased spatial summation of rods that occurs with larger stimulus size, thus increasing retinal sensitivity.[46] The former finding would be due to the increase in rod density with increased eccentricity, normal maximal rod density being distributed in a ring approximately 10° from the foveal center.[47]

We also found that in three of the four conditions tested, achromats had significantly faster recovery of sensitivity than normals, the exception being with a larger, more central stimulus. It is of note that this testing condition set (i.e., larger, more central stimulus) resulted in both the highest final threshold and the slowest rate of sensitivity recovery in the achromat group, although the rate constants did not reach significant difference between the four conditions in either the normal or achromat group (Kruskal-Wallis test; achromats $P = 0.079$; normals $P = 0.503$). That achromats may adapt to scotopic conditions faster than normals has been documented previously,[20,48-50] although it has been proposed that this apparent difference may be due to increased blinking due to photophobia during light adaptation, resulting in patients starting to dark-adapt from a different initial state to that of normal observers.[49] However, given the less intense adaptation light used in our study, this confounder is likely to be mitigated against in our achromat group. Whether faster dark adaptation in achromats compared with normals, when observed, is indeed due to differences in relative adaptation states, or aberrant retinal[51] or higher-order[52] processing remains to be elucidated. However, we also found, in one testing condition, no significant difference between the rate constants in normals and achromats, which would be in agreement with the findings of Simunovic et al.[22] In other retinal diseases, such as fundus albipunctatus and vitamin A deficiency, final DA thresholds are normal but the rate of DA is slowed.[53] The slower rate of DA in these diseases is thought to be mediated on a cellular level by a limitation in the amount of 11-*cis* retinal delivered to rod outer segments[38]; whether in ACHM similar cellular mechanisms are involved, due to photoreceptor (and possibly associated RPE) dysfunction, but are further complicated by other factors such as those mentioned above, is not yet clear. The finding of an elevated final threshold in achromats in some testing conditions may indicate that not all of the rod photoreceptors are functioning normally. None of the achromat subjects had evidence of a biphasic DA curve, which given their lack of any evident cone function on psychophysical and electrophysiological testing, and the low intensity of the adaptation light, is as would be expected.

One possible explanation as to why the more central stimulus location reveals both the lowest final sensitivity relative to normals, and the slowest rates of recovery among the achromat group, may be related to cone density, given that cones are normally more numerous at the more central stimulus location compared with more peripherally.[47] There may be morphologic and/or functional changes in rods attempting to infill spaces no longer fully occupied by functional cones, or anomalies in post receptoral circuitry resulting from nonfunctional cones. Hence, any deleterious effect on rods from a cone dysfunction disease such as ACHM might be more evident centrally, where there would have normally been a greater numbers of functional cones.

If we accept that, in some testing conditions at least, achromats have significantly higher DA final thresholds than normals, this raises the question of whether the rod system in ACHM is functionally entirely normal.[2,16] There have been studies reporting abnormalities in the rod-ERG in some ACHM patients.[3,5,54-56] Our study also suggests that, in some testing conditions, the rod system is less sensitive, in terms of final DA thresholds, than in normals. The reason for this is not clear. It is proposed that, in rod-cone dystrophies, cones may suffer progressive loss from a 'bystander effect' in primary rod disorders,[3] and indeed a rod-derived cone viability factor has been identified.[57] In view of the evidence of degeneration in some individuals with ACHM, it may be that there is some alteration to either the rod photoreceptors themselves, or the neural pathways that subserve them.[56] In support of the latter hypothesis, Haverkamp et al.[51] have shown that in *cnga3*$^{-/-}$ mice, ectopic synapses can be formed between rods and cone bipolar cells. Subnormal rod specific electrophysiological responses have also been documented in other cone dysfunction syndromes, such as Oligocone Trichromacy[58] and X-linked blue-cone monochromatism; rods in the latter condition have also been shown to have minor inner and outer segment abnormalities on imaging.[59] Although there is evidence that primary cone necrosis can promote the secondary apoptosis of healthy rod photoreceptors,[60] there is still much that remains unclear regarding the effect of cone loss on rod function.

The use of advanced imaging techniques such as adaptive optics scanning light ophthalmoscopy (AOSLO), which directly visualizes both the rod and cone photoreceptor mosaic in vivo,[61] is beginning to shed light on photoreceptor integrity in ACHM. The evidence to date suggests that achromats possess residual numbers of variably reflective cones, albeit to a variable degree between patients.[62,63] It will be interesting to establish whether there are any structural rod abnormalities on AOSLO that may correlate with the functional rod impairment suggested by our DA threshold measurements.

We also found that there was no significant difference in the final thresholds or rate constants between the three genotypes. This included comparisons for the patient with the *GNAT2* variant, which is of interest as there is some recent evidence that this genotype may exhibit a milder phenotype as assessed by AOSLO.[64] However, more *GNAT2* patients would need to undergo DA assessments before any conclusions could be drawn.

In three of the four testing condition sets there was no statistically significant correlation between final threshold and rate constant. However, this relationship was significantly positively correlated in at least one of the condition sets (9,9 position, size III stimulus), and the P values approached statistical significance in a further two condition sets (3,3 position, size III stimulus [$P = 0.0503$], and 3,3 position, size V stimulus [$P = 0.06$]). This may suggest that achromat subjects with higher final thresholds dark-adapt to those thresholds more quickly than achromats with lower final thresholds. However, whether this apparent faster rate of DA, when observed, is real or artifactual remains, for reasons stated above, unclear. Individual ACHM subjects that had lower final thresholds tended to do so over all four testing conditions, as did those with higher final thresholds.

One potential limitation of this study was that, although the mean ages of the normal and achromat groups were not significantly different, the patients and normals were not exactly age-matched, and there was a larger range of ages in the achromat group. Dark-adaptation functions, including final thresholds and time constants, deteriorate with age in normals,[65] and there is a current debate over whether achromatopsia itself might be progressive in nature.[66] However, although our achromat group had four patients who were older than the oldest normal subject, it also contained three patients who were younger than the youngest normal subject

by a similar number of years. Given this fact, and that the relationship between DA parameters and age is approximately linear,[65] it is plausible that any losses in sensitivity in the older-than-normal-group patients would be countered by gains in the younger-than-normal-group patients, and therefore have minimal age-related effect on our findings overall.

A further potential limitation concerns the calculated rate constants; although it is believed that complete achromats lack functional cones, there is evidence that a minority of patients have residual cone function.[41,54,55] Individuals with this incomplete form of ACHM retain residual color vision detected by sensitive psychophysical tests.[54,67] Although the results of our testing with both the Ishihara and HRR pseudoisochromatic plates, along with typical ERG recordings, revealed a lack of detectable cone function, more detailed psychophysical testing would be required in order to exclude the possibility of any remaining cone function. Likewise, for our normals, although the adaptation light approximates the minimum brightness for photopic, cone-dependent vision, we cannot fully exclude a cone-dependent contribution to the DA rate constants in the early phase of the sensitivity recovery, even though DA curves previously measured in normals with light adaptation intensities similar to those used here have been shown to be monophasic in nature.[36]

The ability to coregister data from more than one modality will aid detailed phenotyping and monitoring of potential treatment responses. Adaptive optics imaging is likely to be highly applicable to such detailed multimodal assessment and monitoring of patients, especially given that AO imaging has been show to detect changes in photoreceptors that appear normal using conventional imaging modalities.[68,69] It would be of interest to obtain AOSLO images of the photoreceptor mosaic at the corresponding retinal locations tested in our study in both the ACHM patients and normals, in order to probe any detailed local/cellular structure-function correlations between AOSLO parameters (such as photoreceptor size and densities, topographical distribution, and reflectance) and the DA thresholds, as well as assess how any such correlates may change over time.

Regarding the diverging reports concerning DA thresholds in ACHM, our study suggests that the location and size of the stimulus used in DA measurements may be one of the determining factors as to whether the DA thresholds measured are normal or not, which may partly account for the variable findings of previous studies. Another important potential confounder in previous studies is the general lack of a molecular diagnosis of the tested patients, in contrast to our genetically proven patients, with some of the previously reported patients possibly having other cone dysfunction syndromes than ACHM, including S-cone monochromacy.

We have demonstrated that there may be optimum conditions in DA testing that accentuate the relative difference between achromats and normals. If one accepts that these observed differences are predominantly due to rod-system dysfunction in ACHM, it might prove judicious to use these more differentiating conditions for final DA threshold measurements (such as a larger, more centrally located stimulus) in any interventional trial, in order to be able detect any improvement or further compromise in rod function post intervention. Moreover, the shorter testing time and less intense adaptation light will allow scotopic function to be more readily and efficiently probed in other retinal diseases, as well as allowing frequent, less distressing testing of patients (which may include young children) involved in treatment trials. The coregistering of DA data with other imaging modalities such as fundus autofluorescence imaging and AOSLO of the retinal location tested, may also shed further light on the underlying mechanisms of the different thresholds measured, and aid in patient monitoring after treatment.

References

1. Michaelides M, Hunt DM, Moore AT. The cone dysfunction syndromes. *Br J Ophthalmol*. 2004;88:291–297.

2. Andréasson S, Tornqvist K. Electroretinograms in patients with achromatopsia. *Acta Ophthalmol*. 1991;69:711–716.

3. Khan NW, Wissinger B, Kohl S, Sieving PA. CNGB3 achromatopsia with progressive loss of residual cone function and impaired rod-mediated function. *Invest Ophthalmol Vis Sci*. 2007;48:3864–3871.

4. Wissinger B, Jägle H, Kohl S, et al. Human rod monochromacy: linkage analysis and mapping of a cone photoreceptor expressed candidate gene on chromosome 2q11. *Genomics*. 1998;51:325–331.

5. Sundin OH, Yang JM, Li Y, et al. Genetic basis of total colour blindness among the Pingelapese islanders. *Nat Genet*. 2000; 25:289–293.

6. Kohl S, Baumann B, Rosenberg T, et al. Mutations in the cone photoreceptor g-protein α-subunit gene GNAT2 in patients with achromatopsia. *Am J Hum Gen*. 2002;71:422–425.

7. Chang B, Grau T, Dangel S, et al. A homologous genetic basis of the murine cpfl1 mutant and human achromatopsia linked to mutations in the PDE6C gene. *Proc Natl Acad Sci U S A*. 2009; 106:19581–19586.

8. Kohl S, Coppieters F, Meire F, et al. A Nonsense mutation in PDE6H causes autosomal-recessive incomplete achromatopsia. *Am J Hum Genet*. 2012;91:527–532.

9. Johnson S, Michaelides M, Aligianis IA, et al. Achromatopsia caused by novel mutations in both CNGA3 and CNGB3. *J Med Genet*. 2004;41:20e–20.

10. Alexander JJ, Umino Y, Everhart D, et al. Restoration of cone vision in a mouse model of achromatopsia. *Nat Medicine*. 2007;13:685–687.

11. Komáromy AM, Alexander JJ, Rowlan JS, et al. Gene therapy rescues cone function in congenital achromatopsia. *Hum Mol Genet*. 2010;19:2581–2593.

12. Michalakis S, Mühlfriedel R, Tanimoto N, et al. Restoration of cone vision in the CNGA3−/− mouse model of congenital complete lack of cone photoreceptor function. *Mol Ther*. 2010;18:2057–2063.

13. Carvalho LS, Xu J, Pearson RA, et al. Long-term and age-dependent restoration of visual function in a mouse model of CNGB3-associated achromatopsia following gene therapy. *Hum Mol Genet*. 2011;20:3161–3175.

14. Wen R, Tao W, Li Y, Sieving PA. CNTF and retina. *Progr Retin Eye Res*. 2012;31:136–151.

15. Rushton W. Dark-adaptation and the regeneration of rhodopsin. *J Physiol*. 1961;156:166–178.

16. Kelly JP, Crognale MA, Weiss AH. ERGs, cone-isolating VEPs and analytical techniques in children with cone dysfunction syndromes. *Doc Ophthalmol*. 2003;106:289–304.

17. Hess R, Nordby K. Spatial and temporal limits of vision in the achromat. *J Physiol*. 1986;371:365–385.

18. Nordby K, Stabell B, Stabell U. Dark-adaptation of the human rod system. *Vision Res*. 1984;24:841–849.

19. Hess RF, Sharpe LT, Nordby K. *Night Vision: Basic, Clinical and Applied Aspects*. Cambridge: Cambridge University Press; 1990.

20. Rushton W. Rhodopsin measurement and dark-adaptation in a subject deficient in cone vision. *J Physiol*. 1961;156:193–205.

21. Fuortes M, Gunkel R, Rushton W. Increment thresholds in a subject deficient in cone vision. *J Physiol*. 1961;156:179–192.

22. Simunovic MP, Regan BC, Mollon J. Is color vision deficiency an advantage under scotopic conditions? *Invest Ophthalmol Vis Sci*. 2001;42:3357–3364.

23. Sloan LL. Congenital achromatopsia: a report of 19 cases. *JOSA*. 1954;44:117–128.

24. Frey RG, Gordesch J, Heilig P, Thaler A. Dark adaptation in achromats (mathematical analysis) [in German]. *Albrecht Von Graefes Arch Klin Exp Ophthalmol*. 1975;196:299–302.

25. Hess R, Mullen K, Sharpe L, Zrenner E. The photoreceptors in atypical achromatopsia. *J Physiol*. 1989;417:123–149.

26. Blackwell H, Blackwell O. Rod and cone receptor mechanisms in typical and atypical congenital achromatopsia. *Vision Res*. 1961;1:62–107.

27. Sharpe LT, Stockman A, Jagle H, Nathans J. Opsin genes, cone photopigments and colourblindness. In: Gegenfurtner KR, Sharpe LT, eds. *Color Vision: From Genes to Perception*. Cambridge: Cambridge University Press; 2001.

28. Rüther K, Sharpe L, Zrenner E. Dual rod pathways in complete achromatopsia. *Ger J Ophthalmol*. 1994;3:433.

29. Byrne A, Hilbert DR. *Readings on Color: The Science of Color. Volume 2*. Cambridge: The MIT Press; 1997.

30. Hecht S, Shlaer S, Smith EL, Haig C, Peskin JC. The visual functions of the complete colorblind. *J Gen Physiol*. 1948;31:459.

31. Sloan LL, Feiock K. Acuity-luminance function in achromatopsia and in progressive cone degeneration: factors related to individual differences in tolerance to bright light. *Invest Ophthalmol Vis Sci*. 1972;11:862–868.

32. Farkas Á, Wenzel K, Vámos R, Gyory J. A congenitalis achromatopsia diagnosztikai és differenciáldiagnosztikai megközelítése két klinikai eset kapcsán. *Szemeszet*. 1999; 136:187–192.

33. Steinmetz RL, Haimovici R, Jubb C, Fitzke FW, Bird AC. Symptomatic abnormalities of dark adaptation in patients with age-related Bruch's membrane change. *Br J Ophthalmol*. 1993;77:549–554.

34. Heijl PB. *The Field Analyzer Primer: Effective Perimetry*. 4th ed. Oberkochen, Germany: Carl Zeiss Meditec; 2012.

35. Alexander KR, Fishman GA. Prolonged rod dark adaptation in retinitis pigmentosa. *Br J Ophthalmol*. 1984;68:561–569.

36. Hecht S, Haig C, Chase AM. The influence of light adaptation on subsequent dark adaptation of the eye. *J Gen Physiol*. 1937;20:831–850.

37. Thiadens AAHJ, den Hollander AI, Roosing S, et al. Homozygosity mapping reveals PDE6C mutations in patients with early-onset cone photoreceptor disorders. *Am J Hum Genet*. 2009;85:240–247.

38. Lamb TD, Pugh EN Jr. Phototransduction, dark adaptation, and rhodopsin regeneration the proctor lecture. *Invest Ophthalmol Vis Sci*. 2006;47:5137–5152.

39. Goldstein EB. *Sensation and Perception*. Belmont: Cengage Learning; 2013.

40. Kohl S, Varsanyi B, Antunes GA, et al. CNGB3 mutations account for 50% of all cases with autosomal recessive achromatopsia. *Eur J Hum Genet*. 2005;13:302–308.

41. Wissinger B, Gamer D, Jägle H, et al. CNGA3 mutations in hereditary cone photoreceptor disorders. *Am J Hum Genet*. 2001;69:722–737.

42. Aligianis I, Forshew T, Johnson S, et al. Mapping of a novel locus for achromatopsia (*ACHM4*) to 1p and identification of a germline mutation in the α subunit of cone transducin (*GNAT2*). *J Med Genet*. 2002;39:656–660.

43. Kohl S, Marx T, Giddings I, et al. Total colour blindness is caused by mutations in the gene encoding the α-subunit of the cone photoreceptor cGMP-gated cation channel. *Nat Genet*. 1998;19:257–259.

44. Kohl S, Baumann B, Broghammer M, et al. Mutations in the CNGB3 gene encoding the β-subunit of the cone photoreceptor cGMP-gated channel are responsible for achromatopsia (ACHM3) linked to chromosome 8q21. *Hum Mol Genet*. 2000; 9:2107–2116.

45. Sundaram V, Wilde C, Aboshiha J, et al. Retinal structure and function in achromatopsia: implications for gene therapy. *Ophthalmology*. 2014;121:234–245.

46. Bartlett NR. *Vision and Visual Perception*. New York: John Wiley and Sons, Inc.; 1965.

47. Curcio CA, Sloan KR, Kalina RE, Hendrickson AE. Human photoreceptor topography. *J Comp Neurol*. 1990;292:497–523.

48. Sakitt B. Psychophysical correlates of photoreceptor activity. *Vision Res*. 1976;16:129–140.

49. Sharpe LT, Nordby K. The photoreceptors in the achromat. In: Hess RF, Sharpe L, Nordby K, eds. *Night Vision: Basic, Clinical, and Applied Aspects*. Cambridge: Cambridge University Press; 1990:335–389.

50. Krill A, Deutman A, Fishman M. The cone degenerations. *Doc Ophthalmol*. 1973;35:1–80.

51. Haverkamp S, Michalakis S, Claes E, et al. Synaptic plasticity in CNGA3–/– mice: cone bipolar cells react on the missing cone input and form ectopic synapses with rods. *J Neurosci*. 2006; 26:5248–5255.

52. Baseler HA, Brewer AA, Sharpe LT, Morland AB, Jägle H, Wandell BA. Reorganization of human cortical maps caused by inherited photoreceptor abnormalities. *Nat Neurosci*. 2002;5: 364–370.

53. Lamb TD, Pugh EN Jr. Dark adaptation and the retinoid cycle of vision. *Prog Retin Eye Res*. 2004;23:307–380.

54. Genead MA, Fishman GA, Rha J, et al. Photoreceptor structure and function in patients with congenital achromatopsia. *Invest Ophthalmol Vis Sci*. 2011;52:7298–7308.

55. Nishiguchi KM, Sandberg MA, Gorji N, Berson EL, Dryja TP. Cone cGMP-gated channel mutations and clinical findings in patients with achromatopsia, macular degeneration, and other hereditary cone diseases. *Hum Mutat*. 2005;25:248–258.

56. Moskowitz A, Hansen RM, Akula JD, Eklund SE, Fulton AB. Rod and rod-driven function in achromatopsia and blue cone monochromatism. *Invest Ophthalmol Vis Sci*. 2009;50:950–958.

57. Léveillard T, Sahel J-A. Rod-derived cone viability factor for treating blinding diseases: from clinic to redox signaling. *Sci Transl Med*. 2010;2:26ps16.

58. Andersen MK, Christoffersen NL, Sander B, et al. Oligocone trichromacy: clinical and molecular genetic investigations. *Invest Ophthalmol Vis Sci*. 2010;51:89–95.

59. Cideciyan AV, Hufnagel RB, Carroll J, et al. Human cone visual pigment deletions spare sufficient photoreceptors to warrant gene therapy. *Hum Gene Ther*. 2013;24:993–1006.

60. Cho K-I, Haque M, Wang J, et al. Distinct and atypical intrinsic and extrinsic cell death pathways between photoreceptor cell types upon specific ablation of Ranbp2 in cone photoreceptors. *PLoS Genet*. 2013;9:e1003555.

61. Dubra A, Sulai Y, Norris JL, et al. Noninvasive imaging of the human rod photoreceptor mosaic using a confocal adaptive optics scanning ophthalmoscope. *Biomed Opt Express*. 2011;2:1864–1876.

62. Carroll J, Choi SS, Williams DR. In vivo imaging of the photoreceptor mosaic of a rod monochromat. *Vision Res*. 2008;48:2564–2568.

63. Merino D, Duncan JL, Tiruveedhula P, Roorda A. Observation of cone and rod photoreceptors in normal subjects and patients using a new generation adaptive optics scanning laser ophthalmoscope. *Biomed Opt Express*. 2011;2:2189–2201.

64. Dubis AM, Cooper RF, Aboshiha J, et al. Genotype-dependent variability in residual cone structure in achromatopsia: toward developing metrics for assessing cone health. *Invest Ophthalmol Vis Sci*. In press.

65. Jackson GR, Owsley C, McGwin G Jr. Aging and dark adaptation. *Vision Res*. 1999;39:3975–3982.

66. Aboshiha J, Dubis AM, Cowing J, et al. A prospective longitudinal study of retinal structure and function in achromatopsia. *Invest Ophthalmol Vis Sci*. 2014;50:5733–5743.

67. Pokorny J, Smith VC, Pinckers A, Cozijnsen M. Classification of complete and incomplete autosomal recessive achromatopsia. *Graefe's Archive for Clinical and Experimental Ophthalmology*. 1982;219:121–130.

68. Stepien KE, Han DP, Schell J, Godara P, Rha J, Carroll J. Spectral-domain optical coherence tomography and adaptive optics may detect hydroxychloroquine retinal toxicity before symptomatic vision loss. *Trans of the Am Ophthalmol Soc*. 2009;107:28.

69. Rha J, Dubis AM, Wagner-Schuman M, et al. Spectral domain optical coherence tomography and adaptive optics: imaging photoreceptor layer morphology to interpret preclinical phenotypes. In: Anderson RE, Hollyfield JG, LaVail MM, eds. *Retinal Degenerative Diseases*. New York: Springer; 2010:309–316.